

Hydration Energies of Divalent Metal Ions, $\text{Ca}^{2+}(\text{H}_2\text{O})_n$ ($n = 5-7$) and $\text{Ni}^{2+}(\text{H}_2\text{O})_n$ ($n = 6-8$), Obtained by Blackbody Infrared Radiative Dissociation

Sandra E. Rodriguez-Cruz, Rebecca A. Jockusch, and Evan R. Williams*

Department of Chemistry, University of California Berkeley, California 94720

Received March 4, 1998

Metal ions play an important role in the function of many metalloenzymes. For example, the interactions of regulatory proteins such as calmodulin with other proteins depend on whether Ca^{2+} is specifically bound.¹ Studies of metal ion hydration provide information not only about the metal ion chemistry in solution, but can lead to an improved understanding of the structure and function of many biomolecules in which metal ion interactions play a role. The hydration enthalpies of singly charged metal ions in the gas phase have been extensively investigated by using a variety of experimental techniques.² In contrast, gas-phase hydration studies of di- and trivalent metal ions are significantly more limited.³⁻⁵ Kebarle and co-workers measured free energies of hydration for a series of divalent metal ions bound to between 7 and 13 water molecules.^{4b,d} From these values, hydration enthalpies for water molecules in the second solvation shell were estimated. Recently, calculations of successive hydration enthalpies of both inner and outer solvent shell water molecules for several divalent metal ions have been reported.^{6,7} Here, binding energies of water molecules to both divalent calcium and nickel ions are measured by using blackbody infrared radiative dissociation (BIRD) and master equation modeling. These values are considerably lower than MP2 hydration enthalpies reported previously.⁶ They are in better agreement with recently reported B3LYP values calculated with large basis sets.⁷ To our knowledge, these are the first experimental measurements of the binding energy of individual inner shell water molecules to divalent metal ions.

Experimental measurements are performed with an external electrospray ionization source Fourier transform mass spectrom-

eter. This instrument and the BIRD experiments have been described previously.⁸ Hydrated metal ions are generated from $\sim 10^{-4}$ M chloride salt solutions with nano-electrospray ionization. The hydrated ions are trapped and thermalized by using a pulse of N_2 gas (10^{-6} Torr). The ion of interest is mass selected and dissociated for times ranging from 10 to 500 s. At the low pressures during the reaction times ($< 10^{-8}$ Torr), dissociation occurs by absorption of blackbody photons generated by the heated vacuum chamber walls.⁸⁻¹¹ For measurements with hydrated nickel ions, the pressure was $< 3 \times 10^{-8}$ Torr. At this pressure, collisions with background gas (primarily residual N_2) may affect the measured rate constants. Dissociation rate constants are measured as a function of temperature. Under these experimental conditions, the ion population is non-Boltzmann. The threshold dissociation energy (E_0), the thermochemical value of interest, is derived from the measured Arrhenius parameters by master equation modeling.^{9,10} Microcanonical radiative rate constants used in the modeling are calculated from ab initio derived values¹² and varied over a 9-fold range. Microcanonical dissociation rate constants are calculated from RRKM theory and adjusted to provide rapid energy exchange limit A-factors ranging from 10^{14} to $10^{17.2}$ s^{-1} . The range of values of microcanonical rate constants used in the modeling should account for uncertainties in both the calculation of these parameters and the minor effect of collisions with background gas during the nickel experiments. Uncertainties in the modeling as well as those in the experimental values are included in the final error reported for E_0 . The implementation of the master equation model and fitting procedure used to obtain E_0 are described in detail elsewhere.¹⁰

Figure 1 shows the blackbody infrared radiative dissociation data for $\text{Ca}^{2+}(\text{H}_2\text{O})_6$ and $\text{Ni}^{2+}(\text{H}_2\text{O})_6$ at 119 °C. The hydrated calcium ion dissociates more rapidly than nickel. This is consistent with a lower hydration enthalpy due to the larger ionic radius of calcium. For all ions studied, the only dissociation process observed was loss of a single water molecule. Rate constants for dissociation as a function of temperature were measured for all hydrated ions that would dissociate with rate constants between 0.0015 and 0.30 s^{-1} over a temperature range of 22–210 °C. These data are shown in an Arrhenius plot (Figure 2) from which Arrhenius parameters in the zero-pressure limit are obtained (Table 1). Values of E_0 are obtained from master equation modeling of the kinetic data. If the reverse activation barrier for dissociation of these ion–molecule complexes is negligible, then the values of E_0 should be equal to the binding energy or hydration enthalpy at 0 K.

Previous results indicate that accurate dissociation energies of small weakly bound ions can be obtained by using BIRD and master equation modeling.^{10,11} As a further test of this method, the dissociation kinetics of $\text{H}_3\text{O}^+(\text{H}_2\text{O})_n$ ($n = 2, 3$) ions were investigated. The measured zero-pressure limit activation pa-

* To whom correspondence should be addressed.

(1) Creighton, T. E. *Proteins: Structures and Molecular Properties*, 2nd ed.; W. H. Freeman & Co.: New York, 1993.

(2) (a) Keese, R. G.; Castleman, A. W., Jr. *J. Phys. Chem. Ref. Data* **1986**, *15*, 1011–1071. (b) Dzidic, I.; Kebarle, P. *J. Phys. Chem.* **1970**, *74*, 1466–1474. (c) El-Shall, M. S.; Schriver, K. E.; Whetten, R. L.; Meot-Ner (Mautner), M. *J. Phys. Chem.* **1989**, *93*, 7969–7973. (d) Dalleska, N. F.; Honma, K.; Sunderlin, L. S.; Armentrout, P. B. *J. Am. Chem. Soc.* **1994**, *116*, 3519–3528. (e) Marinelli, P. J.; Squires, R. R. *J. Am. Chem. Soc.* **1989**, *111*, 4101–4103. (f) Magnera, T. F.; David, D. E.; Michl, J. *J. Am. Chem. Soc.* **1989**, *111*, 4100–4101. (g) Sanekata, M.; Misaizu, F.; Fuke, K.; Iwata, S.; Hashimoto, K. *J. Am. Chem. Soc.* **1995**, *117*, 747–754. (h) Weinheimer, C. J.; Lisy, J. M. *J. Chem. Phys.* **1996**, *105*, 2938–2941. (i) Beyer, M.; Berg, C.; Görlitzer, H. W.; Schindler, T.; Achatz, U.; Albert, G.; Niedner-Schatteburg, G.; Bondybey, V. E. *J. Am. Chem. Soc.* **1996**, *118*, 7386–7389.

(3) Redeker-Schmelzeisen, G.; Büttfering, L.; Röllgen, F. W. *Int. J. Mass Spectrom. Ion Processes* **1989**, *90*, 139–150.

(4) (a) Jayaweera, P.; Blades, A. T.; Ikononou, M. G.; Kebarle, P. *J. Am. Chem. Soc.* **1990**, *112*, 2452–2454. (b) Blades, A. T.; Jayaweera, P.; Ikononou, M. G.; Kebarle, P. *J. Chem. Phys.* **1990**, *92*, 5900–5906. (c) Blades, A. T.; Jayaweera, P.; Ikononou, M. G.; Kebarle, P. *Int. J. Mass Spectrom. Ion Processes* **1990**, *101*, 325–336. (d) Blades, A. T.; Jayaweera, P.; Ikononou, M. G.; Kebarle, P. *Int. J. Mass Spectrom. Ion Processes* **1990**, *102*, 251–267.

(5) Stace, A. J.; Walker, N. R.; Firth, S. *J. Am. Chem. Soc.* **1997**, *119*, 10239–10240.

(6) (a) Katz, A. K.; Glusker, J. P.; Beebe, S. A.; Bock, C. W. *J. Am. Chem. Soc.* **1996**, *118*, 5752–5763. (b) Glendening, E. D.; Feller, D. *J. Phys. Chem.* **1996**, *100*, 4790–4797.

(7) Pavlov, M.; Siegbahn, P. E. M.; Sandström, M. *J. Phys. Chem. A* **1998**, *102*, 219–228.

(8) Price, W. D.; Schnier, P. D.; Williams, E. R. *Anal. Chem.* **1996**, *68*, 859–866.

(9) Price, W. D.; Schnier, P. D.; Jockusch, R. A.; Strittmatter, E. F.; Williams, E. R. *J. Am. Chem. Soc.* **1996**, *118*, 10640–10644.

(10) Price, W. D.; Schnier, P. D.; Williams, E. R. *J. Phys. Chem. B* **1997**, *101*, 664–673.

(11) Dunbar, R. C.; McMahon, T. B.; Tholmann, D.; Tonner, D. S.; Salahub, D. R.; Wei, D. *J. Am. Chem. Soc.* **1995**, *117*, 12819–12825.

(12) Geometry optimization and force calculations for $\text{M}^{2+}(\text{H}_2\text{O})_n$ were done at the RHF/STO-3G level to obtain vibrational frequencies and transition dipole moments. Values for $\text{H}_3\text{O}^+(\text{H}_2\text{O})_n$ were obtained at the B3LYP/6-31G(d,p) level. $\text{Ni}^{2+}(\text{H}_2\text{O})_n$ was modeled as $\text{Mg}^{2+}(\text{H}_2\text{O})_n$ which has similar $\text{M}^{2+}-\text{H}_2\text{O}$ bond lengths and geometries. $\text{Ni}^{2+}(\text{H}_2\text{O})_6$ was also modeled at the B3LYP/LANL2DZ level. The value of E_0 obtained from master equation modeling is virtually identical with the one obtained by using parameters from $\text{Mg}^{2+}(\text{H}_2\text{O})_6$ modeled at the RHF/STO-3G level. This indicates that substituting Mg^{2+} for Ni^{2+} in the master equation modeling does not significantly affect the resulting value of E_0 .

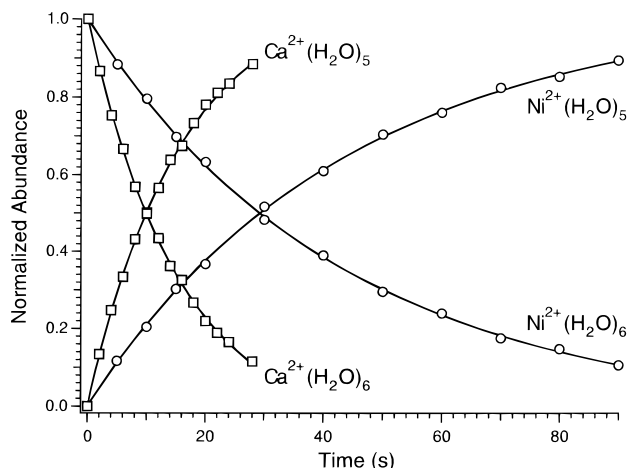


Figure 1. Appearance/depletion curves for the loss of one water molecule from $\text{Ni}^{2+}(\text{H}_2\text{O})_6$ (circles) and $\text{Ca}^{2+}(\text{H}_2\text{O})_6$ (squares) measured by using blackbody infrared radiative dissociation at 119 °C.

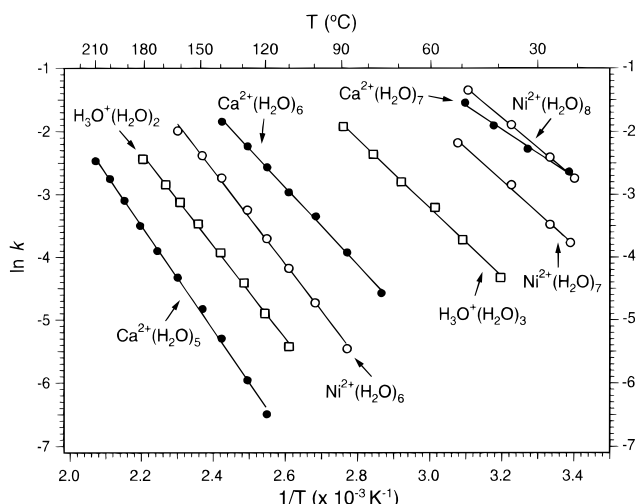


Figure 2. Arrhenius plots for the dissociation of $\text{Ni}^{2+}(\text{H}_2\text{O})_n$ (open circles), $\text{Ca}^{2+}(\text{H}_2\text{O})_n$ (filled circles), and $\text{H}_3\text{O}^+(\text{H}_2\text{O})_n$ (open squares).

Table 1. Measured Zero-Pressure Limit Arrhenius Parameters and E_0 Values Obtained from Master Equation Modeling for Loss of One Water Molecule from $\text{Ni}^{2+}(\text{H}_2\text{O})_n$, $\text{Ca}^{2+}(\text{H}_2\text{O})_n$, and $\text{H}_3\text{O}^+(\text{H}_2\text{O})_n$ along with Previously Reported Hydration Enthalpies

	n	E_a (kcal/mol)	$\log A$	E_0 (kcal/mol)	ΔH^{298} (kcal/mol)
$\text{Ni}^{2+}(\text{H}_2\text{O})_n$	6	14.8 ± 0.1	6.6 ± 0.2	24.1 ± 1.0	
	7	10.1 ± 0.5	5.9 ± 0.3	17.6 ± 0.8	
	8	9.3 ± 0.3	5.7 ± 0.1	17.1 ± 0.7	15.1^b
$\text{Ca}^{2+}(\text{H}_2\text{O})_n$	5	16.5 ± 0.2	6.4 ± 0.1	26.3 ± 1.4	$34.2,^{c,30.1,^d}27.7^e$
	6	12.2 ± 0.2	5.6 ± 0.1	21.9 ± 1.4	$31.8,^{c,27.2,^d}24.7^e$
	7	7.4 ± 0.4	4.3 ± 0.3	16.4 ± 1.2	$21.4,^{i,17.6^e}$
$\text{H}_3\text{O}^+(\text{H}_2\text{O})_n$	2	14.7 ± 0.2	6.0 ± 0.2	19.0 ± 0.4	$22.3,^f19.5,^g21.0,^h$
				18.8 ± 0.2^a	$19.0,^{20.5^j}$
	3	10.8 ± 0.3	5.7 ± 0.2	16.1 ± 0.3	$17.0,^f17.9,^g16.0,^h$ 15.9 ± 0.3^a $17.6,^{16.7^j}$

^a Values obtained with a truncated Boltzmann model. ^b HPMS results from Kebarle and co-workers (ref 4d). ^c MP2 calculations from Bock and co-workers (ref 6a). ^d MP2 calculations from Glendening and Feller (ref 6b). ^e B3LYP calculations from Pavlov and co-workers (ref 7). ^f Kebarle and co-workers (ref 13). ^g Kebarle and co-workers (ref 14). ^h Meot-Ner and Field (ref 15). ⁱ Meot-Ner and Speller (ref 16). ^j Armentrout and co-workers (ref 17).

rameters and values of E_0 obtained from modeling (Table 1) are comparable to those of the hydrated metal ions. From master equation modeling, E_0 values of 19.0 ± 0.4 and 16.1 ± 0.3 kcal/mol are obtained for $n = 2$ and 3, respectively. Nearly identical

values are obtained from the dissociation kinetics of these weakly bound clusters by using the truncated Boltzmann model of Dunbar (Table 1).¹¹ These values are in excellent agreement with those obtained previously with both high-pressure mass spectrometry (HPMS)^{13–16} and energy resolved collisionally activated dissociation (CAD)¹⁷ methods (Table 1). The excellent agreement indicates that the values of E_0 reported here for the hydrated divalent metal ions should have comparable accuracy.

For $\text{Ni}^{2+}(\text{H}_2\text{O})_8$, the value of E_0 (17.1 ± 0.7 kcal/mol) is slightly higher than the value of 15.1 kcal/mol measured by Kebarle and co-workers.^{4d} Kebarle's value is likely to be somewhat low due to effects of clustering which perturb the equilibrium distribution of ions in the HPMS experiment, but the difference in these values is negligible. We obtain a similar value of E_0 for $n = 7$ and 8, but the value for $n = 6$ is significantly higher. The large jump in E_0 indicates that the sixth water molecule is part of the first hydration shell whereas the seventh and eighth water molecules are in the second shell. This is consistent with the known coordination of Ni^{2+} in bulk solution.¹⁸

For $\text{Ca}^{2+}(\text{H}_2\text{O})_n$, the values of E_0 steadily increase by ~ 5 kcal/mol for $n = 7–5$.¹⁹ This is in contrast to the Ni which clearly has a large increase in binding energy at $n = 6$. Both experimental and theoretical studies of Ca^{2+} in solution indicate that 7, 8, and even 9 water molecules can be accommodated in the first solvation shell due to the large ionic radius of calcium.²⁰ Solvation of calcium ions in the protein calmodulin also occurs by interaction with eight oxygen atoms from carbonyl or hydroxyl groups.¹ The values of E_0 obtained for calcium are significantly lower than MP2 calculations of the hydration enthalpy,⁶ but are comparable to B3LYP values reported by Pavlov et al. (Table 1).⁷ The results of Pavlov et al. indicate that the most stable structure of $\text{Ca}^{2+}(\text{H}_2\text{O})_7$ is one in which there are six water molecules in the first shell and one in the second shell. Our measured values are close to the hydration energies calculated for this structure. However, the monotonic decrease in binding energy we observe is somewhat suggestive of a structure in which all seven water molecules are in the first shell.

The binding energies of water to the two divalent metal ions reported here cover the full range of values that can be measured for these ions by using BIRD with the current experimental apparatus. At higher temperatures or with other methods, such as energy resolved CAD, it should be possible to measure binding energies of water to divalent metal ions for even lower extents of hydration. Accurate hydration enthalpies for di- and trivalent metal ions should greatly improve our understanding of interactions of these metal ions both with water and with biomolecules.

Acknowledgment. The authors thank Mr. Martin Beyer for helpful discussions and assistance with the calculations. Financial support was generously provided by the National Science Foundation (CHE-9726183) and the National Institutes of Health (IR29GM50336-01A2, and fellowship support for R.A.J.)

JA980716I

(13) Kebarle, P.; Searle, S. K.; Zolla, A.; Scarborough, J.; Arshadi, M. *J. Am. Chem. Soc.* **1967**, *89*, 6393–6399.

(14) Lau, Y. K.; Ikuta, S.; Kebarle, P. *J. Am. Chem. Soc.* **1982**, *104*, 1462–1469.

(15) Meot-Ner (Mautner), M.; Field, F. H. *J. Am. Chem. Soc.* **1977**, *99*, 998–1003.

(16) Meot-Ner (Mautner), M.; Speller, C. V. *J. Phys. Chem.* **1986**, *90*, 6616–6624.

(17) Dalleska, N. F.; Honma, K.; Armentrout, P. B. *J. Am. Chem. Soc.* **1993**, *115*, 12125–12130.

(18) Gallucci, J. C.; Gerkin, R. E. *Acta Crystallogr.* **1990**, *C46*, 350–354.

(19) Two different structures of $\text{Ca}^{2+}(\text{H}_2\text{O})_7$ were modeled: one with all seven water molecules in the inner shell, the other with six water molecules in the inner shell and one in the outer shell. The range of E_0 values we report for this ion includes the values obtained from both structures.

(20) (a) Hewish, N. A.; Neilson, G. W.; Enderby, J. E. *Nature* **1982**, *297*, 138–139. (b) Floris, F. M.; Persico, M.; Tani, A.; Tomasi, J. *Chem. Phys. Lett.* **1994**, *227*, 126–132.